Emerging Trends in Engineering and Sustainability (ETES) Volume 02 (No. 02), 2026, pp 59-67

Emerging Trends in Engineering and Sustainability (ETES)

https://etes.alnaji-uni.edu.iq

https://doi.org/ 10.65505/ETES-26-0008

ISSN 3105-1723 (Print)
ISSN 3105-1731 (Online)

Impact of Shading Ratio on Silicon Monocrystalline Solar Module Yield and Power Output

Hussein Ahmed Abar[1*]

[1] Department of Energy, College of Engineering, University of Baghdad, Baghdad, Iraq

Article Info

Received: June 08 2026
Revised: June 25 2026
Accepted: June 26 2026
Available online: June 30 2026

Keywords:
Shading
Voltage
Current
Power
Patten

ABSTRACT

Shadows dramatically reduce the solar panel output because individual cells are wired in chains (series). Blocking a single cell blocks the current across the entire chain. While bypass diodes bypass shaded sections, severe shadows can still cause “hot spots,” which permanently damage panels. The proposed work presents an experimental measurement of the impact of shading on monocrystalline power losses. The solar module was exposed to real environmental conditions, with direct solar radiation of 500 W/m² and 80 W/m² at the penumbra shading of the shaded area, and an operating solar module temperature of 25°C at an ambient temperature of 18°C. The Solar Module Analyzer simulator was used in this study, which tested 10 shading patterns. The photovoltaic solar module’s performance in terms of output power and fill factor, and the corresponding efficiency, is greatly affected by shading. The maximum output power drops drastically, often much more than the shaded area percentage would suggest; 25% shading can lead to 60% power loss, and 50% shading can lead to 60% power loss. It is noticeable that there is a sudden change in the behavior of the I-V and P-V characteristic curves at a certain range of open-circuit voltage (9-9.5 V).

1. Introduction

The heaviness (or intensity) of a shadow on a solar module is directly and nonlinearly proportional to the power loss. Shading blocks incoming sunlight (irradiance), which deprives the solar cells of the photons required to generate electricity. Even a small, faint shadow can cause a significant drop in the energy output of a system. The rapid growth of on-grid PV power systems is considered an alternative distributed energy resource [1].

Simple installation and adaptability have led to the widespread use of these systems in urban areas. An effective environmental factor is that shadows from nearby buildings cause outlet energy loss and structural failure [2].

Several studies have been conducted on modeling approaches and shadow impact quantification (definition, classification, and harmful conditions) [3,4]. There is an urgent need for improved technology and design for simulation, supervision, and control to avoid power loss in PV systems [5-7]. The configuration of solar arrays is considered one of the best solutions to mitigate the shadow effect on solar array system performance [8].

Several external factors, such as trees, buildings, or clouds, are among the significant parameters for power loss in PV array systems [9]. studied the thermodynamic and electrical parameters of 75 W solar panels with different geometric shading ratios [10]—three types of shading ratio: cells, horizontal, and vertical shading at various percentages. The greatest power loss was thus 69.92% in cellular, 66.93%

in vertical, and 99.98% in horizontal shading at a shading rate of 100% [10]. studied the thermal effect and electrical parameter performance of solar modules under static and dynamic shading. Many studies have focused on mitigating and minimizing the shadow effect and enhancing module performance and efficiency [11]. used reconfiguration procedures to reduce shadow effects in solar PV arrays.

Dynamic reconfiguration approaches are costly, but they can effectively compensate for partial shading and mismatch effects in PV arrays compared with static solutions. used the PV array reconfiguration (PVR) method to reduce power losses and maximize the module efficiency caused by the shadow effect.

Many studies have focused on optimizing PV systems for electricity generation [12]. investigated intelligent control to optimize a PV system in varying atmospheric conditions [13]. Different lines, artificial neural networks (ANNs), and adaptive neuro-fuzzy inference systems (ANFIS) have been utilized to describe machine learning methods to optimize the PV system.

The proposed method can increase the potential of solar cells by at least 70% and can serve as a model for future generations of office and residential construction. To maximize the solar array system performance, some researchers have addressed the effects of tilt and azimuth [14]. The research study showed that shading ratios of 40-60% potentially increased the temperature of the shaded portion from 25 to 105 °C [15]. A hotspot at 145 °C was observed in this study, along with variations in cell characteristics during shading [16]. In addition, partial shading results in multiple peaks in the module characteristics, which directly impacts the output generation and reduces the life expectancy of the PV module 36 [17]. Using this technique, the hotspot temperature dropped from 55 °C to 35 °C, and the output power increased by 5.3% [18]. The present work aims to evaluate the impact of shading on the power drop and yield productivity of a photovoltaic monocrystalline solar module at a solar irradiance of 500 W/m².

2. Experimental measurements and device

A 30 W monocrystalline silicon solar panel was tested in the Energy Engineering Laboratory at the University of Baghdad from November 1, 2025, to January 31, 2026. A wireless weather sensor was used. The solar irradiance was approximately 500 W/m², the average wind speed was 3.4 m/s, the ambient temperature was around 18°C, and the relative humidity ranged between 30% and 40%, at latitude 33.33°N and longitude 44.43°E. The experimental measurements focused on the effect of static partial shading on solar module performance. Shading was applied using a piece of cardboard, and 19 different shading patterns were tested, assuming an incident irradiance of 80 W/m² on the shaded area.

2.1 The monocrystalline silicon solar module

A monocrystalline silicon solar panel was tested under outdoor operating conditions. Table 1 shows the panel's technical specifications, as provided by the manufacturer under Standard Test Conditions (STC). The manufacturer's data, including values for the short-circuit current (I_{sc}), open-circuit voltage (V_{oc}), maximum current (I_{max}), maximum voltage (V_{max}), and maximum power (P_{max}), were used in the panel's calibration process. These values are marked at the back of the panel. The test results showed a high degree of convergence between the measured values, with a standard deviation of approximately 0.05, indicating the consistency and accuracy of the measurements.

Table 1. Module specifications at STC, as presented by the manufacturer.

Area, m²	Open-circuit voltage, V	Short-circuit current, A	Peak power, W	Peak voltage, V	Peak current, A	No. of cells	Production data
0.26	22	1.9	30	17.0	1.76	36	2022

2.2 Wireless Weather Sensor with GPS

The Wireless Weather Sensor is a comprehensive tool designed for monitoring various environmental factors, as demonstrated in Figure 1. It integrates multiple sensors into a single unit, allowing the collection of 19 distinct measurements. The sensor can be used in logging mode with the Weather Vane Accessory for extended monitoring or as a portable device for studying microclimates and local environmental changes. The gathered data can be wirelessly transmitted to most devices, including classroom dashboards, aiding time-sensitive group activities.

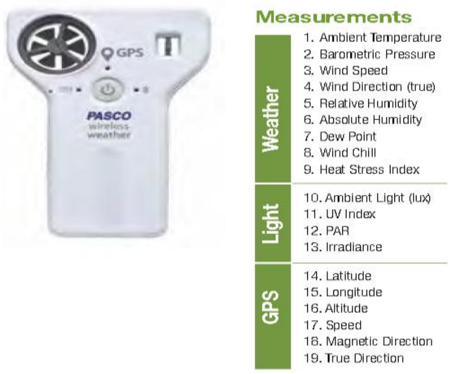

Figure 1. Wireless weather sensor with 19 measurements.

2.3 The current-voltage (I-V) and power-voltage (P-V) tracers

The Solar Module Analyzer (Prova 200) is an electrical device that applies different loads to obtain the solar module characteristic curves (I-V and P-V). The current-voltage characteristic curve is drawn by applying load 0-∞ Ω, the corresponding Power-Voltage will be available with this load (Prova 200 calibrated according to standard procedure supplied by the manufacturer). For a voltage range of 10 V to 1000 V and a corresponding current range of 20-30 A, the characteristic curve can be measured. The uncertainty in the measurement of power, current, and voltage is should be within 1%. Solar module analyzer (Prova 200) is a portable instrument used for measuring and analyzing power quality parameters has a maximum voltage measurement range of 0–1000 V and a maximum current measurement range of 0.25–600 A. Solar module analyzer (see Figure 2) was used to test the characteristics (V_{oc}, I_{sc} , V_m , I_m and P_m), as well as the solar panel's efficiency and fill factor. Prova 200 generates the I-V curve by changing the load from 0 Ω (0, I_{sc}) to ∞ Ω (V_{oc},0) with a time of 10s. The device has an option to set the values for both solar radiation rate (TES-1333R solar power meter) and solar module operating temperature (TPM-10 Temperature sensor), as shown in Figure 2.

2.4 Experimental procedure

The readings were obtained on sequential days. Winter conditions constrained data collection efforts during this period. Figure 1 shows a completed cell testing assembly placed under natural sunlight for the partial shading experiment. The static shading block is achieved using a piece of cardboard for 10 shaded pattern cases of solar module cells, at a distance of about half a meter from the solar module. These shaded pattern cases are summarized in Figure 3.

(a) (b) (c)

Figure 2. Measuring devices, from left to right: (a)TPM-10 Temperature sensor, (b) TES-1333R solar power meter, and (c) Prova 200 Solar Module Analyzer, respectively.

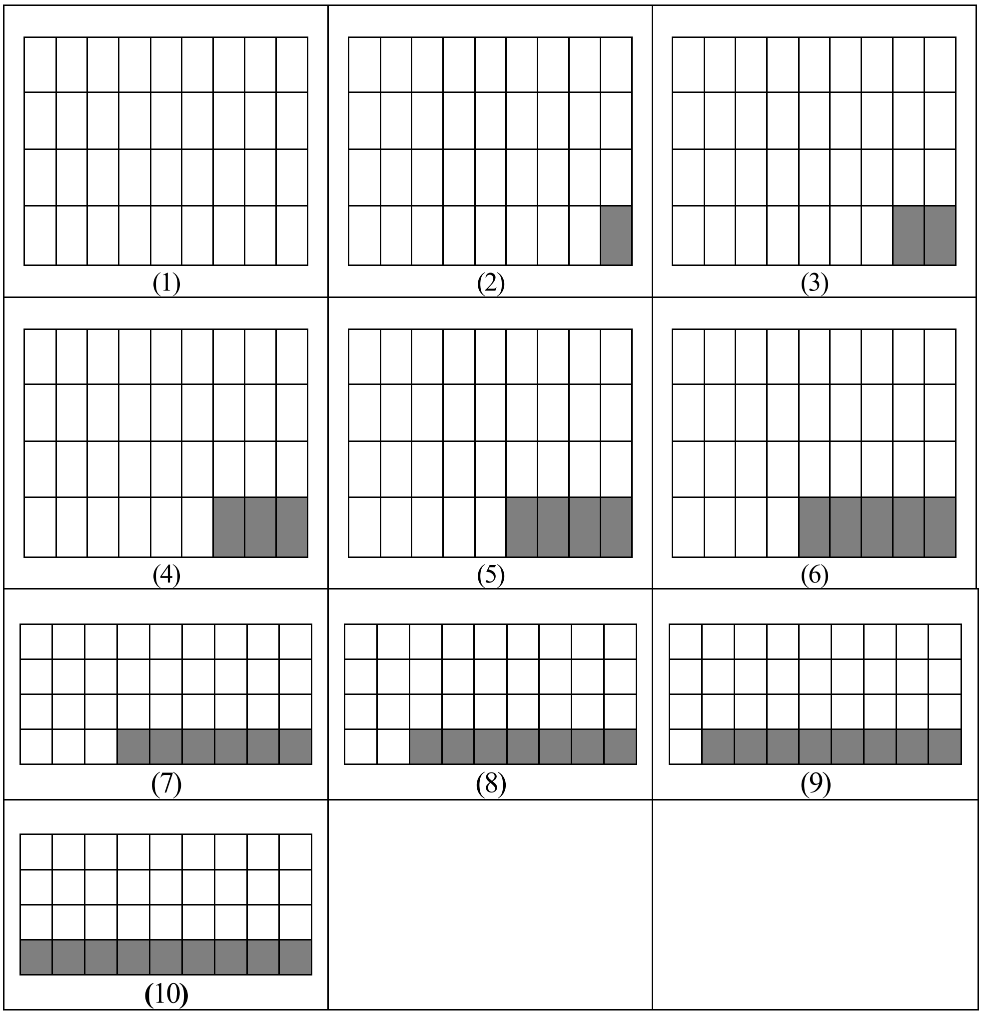

Figure 3. Static 10 shadow pattern cases

Figure 4. Photograph of the experiment apparatus.

The Prova 200 was connected to a computer to transfer the data directly to an Excel spreadsheet.

The operation was carried out during the specified time period from 9:30 am to 12:30 pm on randomly selected days. The measurement conditions were direct solar radiation of about 500 W/m² and 80 W/m² at penumbra shading, with a solar module operating temperature of 25°C at an ambient temperature of 18°C. Furthermore, a solar module analyzer needs 10 seconds to make I-V and P-V measurements with a variable load 0-∞Ω Moreover, it is already the experiment apparatus in outdoor conditions (steady state), and the variables would not change within 10 seconds. The module is cleaned of dirt or dust before the experimental measurements. All measurements were taken when solar radiation was as constant as possible (A flexible mounting frame that can be manually adjusted to ensure that the incident radiation remains within the specified range). Using a solar module analyzer, the temperature of the module's back side was recorded, and a current-voltage scan was performed, with the resulting data stored on a computer (see Figure 2).

The previous steps were repeated more than one time for a specific temperature, especially for a partly cloudy day (take the accurate measurements, not the average; if there is a sudden fluctuation in temperature or irradiance of more than 200, make a default case). The experiment was carried out on a 30 W solar module. The solar module consists of 36 cells connected in series. The module has a tilt angle range of 30° - 35° (use a fixed stand).

3. Results and discussions

3.1 Electric solar module parameters

Solar monocrystalline photovoltaic solar module parameters: V_{oc} (V), I_{sc} (A), V_{max} (V), I_{max} (A), P_{max} (W), FF, and η (%) with 25 °C solar module operation temperature and 500 W/m² solar irradiances and solar radiation at a shadowed area of 80 W/m² as shown in Table 2. Table 2 presents the case study of shadowed solar cells for teens. Partial shading causes a sudden decrease in total output power, with a drop in current and the appearance of multiple peaks in the power-voltage (P-V) curve, leading to significant changes in the electrical characteristics of the solar panel.

The short-circuit current is more affected by shading than other parameters because the solar cells in a panel are typically connected in series. Therefore, the total current in the series is determined by the level of the least illuminated (shaded) cell, which is essentially the "weakest link" in the chain. In contrast, the open-circuit voltage is less affected by partial shading than the current, because it depends primarily on the cell material and panel temperature rather than on the overall illumination intensity across the panel.

It is noted that no significant change occurs in the value of the short-circuit current (Isc) during cases 1 to 10 as shown in Table 3. It is noticeable in the Table 3 that the short circuit voltage (V_{oc}) value changes slightly with all shaded (1-10) cases of misleading. The noticeable drop in voltage is directly related to the percentage of the shaded area, which is expressed as the highest current (V_m). This drop usually only appears when a large part of the panel is shaded or when the entire solar string is affected. The maximum power (P_{max}) at solar radiation intensity 500W/m² is 20.95W (case 1), while the minimum corresponding one is 8.326 W (case 10) at the same solar irradiance. The maximum open voltage is equal to 20.91 V (case 2), maximum short current is equal to 1.46 A (case 2).

Table 2. Electrical parameters of monocrystalline photovoltaic solar module at solar radiation of **500**W/m² and solar radiation at shadowed area 80 W/m²

Case No.	V_{oc}, V	I_{sc},A	V_m,V	I_m,A	P_m,W	FF	η, %
Case 1	20.91	1.46	17.17	1.221	20.95	0.686	15.8
Case 2	21.03	1.26	8.02	1.071	8.598	0.324	6.5
Case 3	21.02	1.26	8.03	1.069	8.584	0.322	6.4
Case 4	21.06	1.26	8.14	1.054	8.579	0.323	6.4
Case 5	21.08	1.26	8.13	1.052	8.552	0.321	6.4
Case 6	21.05	1.26	8.11	1.051	8.523	0.321	6.4
Case 7	21.01	1.24	8.058	1.050	8.461	0.321	6.3
Case 8	21.05	1.22	8.043	1.046	8.412	0.322	6.3
Case 9	20.99	1.24	8.064	1.038	8.370	0.321	6.2
Case10	20.93	1.24	8.123	1.025	8.326	0.321	6.2

3.2 Characteristic curves of solar module

The current-voltage characteristic curves for the shaded case study are shown in Figure 5 and summarized in Figure 6. In contrast, the corresponding power-voltage characteristic curves are shown in Figure 7 and Figure 8. An increase in current leads to higher power output due to increased incident solar radiation. Despite the change in voltage, the current produced by the incident light remains constant with a slight increase. The maximum power output drops drastically, often much more than the shaded area percentage would suggest. The panel's power output drops to about 50% when one of the 36 cells in the solar module is shaded, and this percentage remains almost constant even when one, two, four, or even nine cells are shaded if they are on a horizontal line (from case 1 to case 9). The power-voltage (P-V) curve is usually a single peak, but in the case of partial shading it becomes a curve with several local power peaks, making it difficult for traditional Maximum Power Point Tracking (MPPT) algorithms to determine the true (global) maximum power point. This behavior is consistent across all cases, as there is no single point that represents the maximum power. A sudden change in the behavior of the I–V and P–V characteristic curves is also observed at a specific open-circuit voltage (V_{oc}) value between 9 and 9.5 V. The sudden change in the I-V and P-V characteristic curves is caused by the activation of the bypass diode. At the start of the partial shading event, when the shadow edge moves over the first sub-cells of the module, there is only one maximum power point (MPP), and the global maximum power point (GMPP) voltage is nearly constant near the nominal value (solid curve in Figure 5). When more and more sub-solar cells get shaded, multiple MPPs start to exist on the P-V curve (solid curve in Figure 4). Due to partial shading, a significant drop in the solar array's output power occurs as a result of multiple peaks appearing on the power-voltage (P-V) curve, leading to the emergence of local maximum power points (LMPPs) that can mislead conventional tracking algorithms. The number of maximum power points (MPPs) gradually and steadily increases until it reaches its maximum possible value. This creates a "Global Maximum Power Point" (GMPP) challenge, where output can drop by over 70% if the wrong peak is tracked.

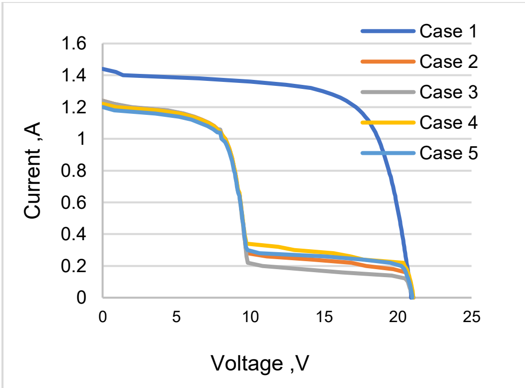

Figure 5. Voltage-current characteristic curve of monocrystalline solar module at different shadow patterns (case1 to case5) with solar radiation 500 W/m², solar radiation at shadowed area 80 W/m² and operating solar module temperature of 25 °C.

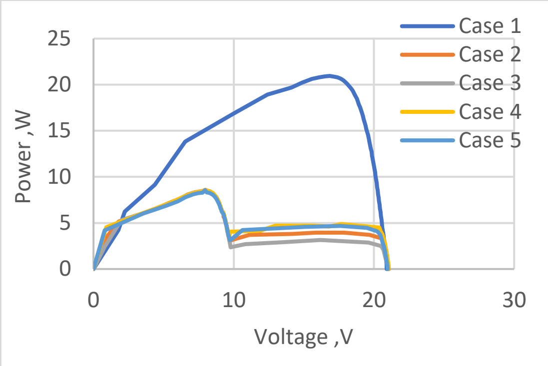

Figure 6. Power-Voltage characteristic curve of monocrystalline solar module at different shadow patterns (case1 to case5) with solar radiation 500 W/m^2, solar radiation at shadowed area 80 W/m^2 and operating solar module temperature of 25 °C.

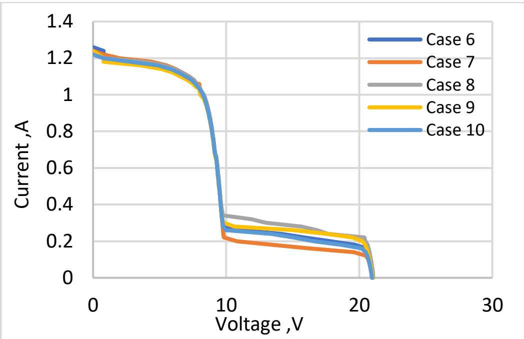

Figure 7. Voltage-current characteristic curve of monocrystalline solar module at different shadow patterns (case6 to case10) with solar radiation 500 W/m², solar radiation at shadowed area 80 W/m² and operating solar module temperature of 25 °C

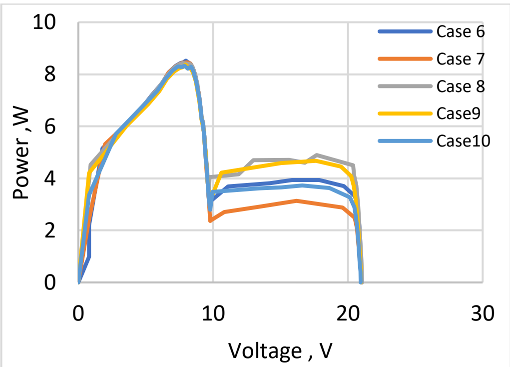

Figure 8. Power-Voltage characteristic curve of monocrystalline solar module at different shadow patterns (case6 to case10) with solar radiation 500 W/m², solar radiation at shadowed area 80 W/m² and operating solar module temperature of 25 °C.

4. Conclusions

This paper presents a moncrystalline solar module that are partially shaded. Solving a set of set of shading ratio. The anaylsis, undertaken under a variety of partial shade settings as well as some uniform conditions. This study focused on analyzing changes in electrical parameters and power drop with different shading ratio on the performance of solar module. Teen different cases of solar module shading patterns were studied, through which the evolution of electrical parameters expressing the unit's performance was obtained, in addition to current-voltage (I–V) and power-voltage (P–V) curves with changing shading ratios. A significant change in the behavior of the current-voltage (I-V) and power-voltage (P-V) curves is observed at a specific open-circuit voltage value between 9 and 9.5 volts, due to the shading effect. This sudden change in characteristic curves is caused by the activation of the bypass diode.

Acknowledgements

The author expresses his appreciation to the lab team in the Department of Energy, College of Engineering, University of Baghdad.

Conflict of interest

The authors declare no conflicts of interest concerning this research.

Funding

No funding was received for conducting this study.

AI Declaration Statement

The authors confirm that the manuscript has been written without the assistance of generative AI or AI-based writing tools.

References

[1] O. M. Toledo, D. O. Filho, A. S. A. C. Diniz, J. H. Martins, and M. H. M. Vale, "Methodology for Evaluation of Grid-Tie Connection of Distributed Energy Resources—Case Study with Photovoltaic and Energy Storage," IEEE Trans. Power Syst., vol. 28, no. 2, pp. 1132–1139, May 2013.

https://doi.org/10.1109/TPWRS.2012.2207971.

[2] A. E. Brooks, D. Cormode, A. D. Cronin, and E. Kam-Lum, "PV System Power Loss and Module Damage Due to Partial Shade and Bypass Diode Failure Depend on Cell Behavior in Reverse Bias," in Proc. IEEE 42nd Photovoltaic Spec. Conf. (PVSC), New Orleans, LA, USA, Jun. 2015, pp. 1–6. https://doi.org/10.1109/PVSC.2015.7356290.

[3] E. Batzelis, P. Georgilakis, and S. Papathanassiou, "Energy Models for Photovoltaic Systems Under Partial Shading Conditions: A Comprehensive Review," IET Renew. Power Gener., vol. 9, no. 4, pp. 340–349, 2015. https://doi.org/10.1049/iet-rpg.2014.0207.

[4] P. L. Hidalgo-Gonzalez, A. E. Brooks, E. S. Kopp, V. P. Lonij, and A. D. Cronin, "String-Level (kW-Scale) I-V Curves from Different Module Types Under Partial Shade," in Proc. 38th IEEE Photovoltaic Spec. Conf. (PVSC), Austin, TX, USA, Jun. 2012, pp. 1442–1447. https://doi.org/10.1109/PVSC.2012.6317868.

[5] J. Bai, Y. Cao, Y. Hao, Z. Zhang, S. Liu, and F. Cao, "Characteristic Output of PV Systems Under Partial Shading or Mismatch Conditions," Sol. Energy, vol. 112, pp. 41–54, 2015. https://doi.org/10.1016/j.solener.2014.09.048.

[6] S. Z. M. Golroodbari, A. C. de Waal, and W. G. J. H. M. van Sark, "Improvement of Shade Resilience in Photovoltaic Modules Using Buck Converters in a Smart Module Architecture," Energies, vol. 11, no. 1, art. no. 250, Jan. 2018. https://doi.org/10.3390/en11010250.

[7] A. Triki-Lahiani, A. B. B. Abdelghani, and I. Slama-Belkhodja, "Fault Detection and Monitoring Systems for Photovoltaic Installations: A Review," Renew. Sustain. Energy Rev., vol. 82, pp. 2680–2692, Feb. 2018. https://doi.org/10.1016/j.rser.2017.09.101.

[8] A. K. Tripathi, M. Aruna, and C. S. Murthy, "Performance of a PV Panel Under Different Shading Strengths," Int. J. Ambient Energy, vol. 40, no. 3, pp. 248–253, 2019. https://doi.org/10.1080/01430750.2017.1388839.

[9] B. Hu, J. Wu, P. Li, W. Sun, and J. Xiao, "Calculating the Shading Reduction Coefficient of Photovoltaic System Efficiency Using the Anisotropic Sky Scattering Model," Glob. Energy Interconnect., vol. 5, no. 4, pp. 375–384, 2022. https://doi.org/10.1016/j.gloei.2022.08.004.

[10] F. Bayrak and H. F. Oztop, "Effects of Static and Dynamic Shading on Thermodynamic and Electrical Performance for Photovoltaic Panels," Appl. Therm. Eng., vol. 169, art. no. 114900, 2020. https://doi.org/10.1016/j.applthermaleng.2020.114900.

[11] S. G. Krishna and T. Moger, "Reconfiguration Strategies for Reducing Partial Shading Effects in Photovoltaic Arrays: State of the Art," Sol. Energy, vol. 182, pp. 429–452, 2019. https://doi.org/10.1016/j.solener.2019.02.057.

[12] K. Osmani, A. Haddad, H. Jaber, T. Lemenand, B. Castanier, and M. Ramadan, "Mitigating the Effects of Partial Shading on PV System Performance Through PV Array Reconfiguration: A Review," Therm. Sci. Eng. Prog., vol. 31, art. no. 101280, 2022. https://doi.org/10.1016/j.tsep.2022.101280.

[13] A. Ba, A. Ndiaye, E. H. M. Ndiaye, and S. Mbodji, "Power Optimization of a Photovoltaic System with Artificial Intelligence Algorithms over Two Seasons in Tropical Area," MethodsX, vol. 10, no. 1, art. no. 101959, 2023. https://doi.org/10.1016/j.mex.2022.101959.

[14] W. Liu, Y. Shen, P. Aungkulanon, M. Ghalandari, B. N. Le, A. Alviz-Meza, and Y. Cárdenas-Escrocia, "Machine Learning Applications for Photovoltaic System Optimization in Zero Green Energy Buildings," Energy Rep., vol. 9, no. 3, pp. 2787–2796, 2023. https://doi.org/10.1016/j.egyr.2023.01.114.

[15] M. Dhimish and P. I. Lazaridis, "An Empirical Investigation on the Correlation Between Solar Cell Cracks and Hotspots," Sci. Rep., vol. 11, no. 1, art. no. 23961,

2021. https://doi.org/10.1038/s41598-021-03498-z.

[16] C. E. Clement, J. P. Singh, E. Birgersson, Y. Wang, and Y. S. Khoo, "Hotspot Development and Shading Response of Shingled PV Modules," Sol. Energy, vol. 207, no. 1, pp. 729–735, 2020. https://doi.org/10.1016/j.solener.2020.06.078.

[17] C. Olalla, M. N. Hasan, C. Deline, and D. Maksimović, "Mitigation of Hotspots in Photovoltaic Systems Using Distributed Power Electronics," Energies, vol. 11, no. 4, art. no. 726, 2018. https://doi.org/10.3390/en11040726.

[18] M. Dhimish, M. Theristis, and V. d'Alessandro, "Photovoltaic Hotspots: A Mitigation Technique and Its Thermal Cycle," Optik, vol. 300, art. no. 171627, 2024. https://doi.org/10.1016/j.ijleo.2024.171627.